

Polarized and Unpolarized Lepton Pair Forward-backward Asymmetries in $\bar{B} \rightarrow \bar{K}_0^*(1430)\ell^+\ell^-$ and $\bar{B} \rightarrow \bar{K}\ell^+\ell^-$ Decays in Two Higgs Doublet Model

F. Falahati^{a*} and H. Abbasi

^a*Physics Department and Biruni Observatory, College of Sciences, Shiraz University, Shiraz 71454, Iran*

In this paper we shall focus on the effects of concrete models such as SM and Model III of 2HDM on the polarized and unpolarized forward-backward asymmetries of $\bar{B} \rightarrow \bar{K}_0^*(1430)\ell^+\ell^-$ and $\bar{B} \rightarrow \bar{K}\ell^+\ell^-$ decays. The obtained results of these decay modes are compared to each other. Also, we obtain the minimum required number of events for detecting each asymmetry and compare them with the number of produced $B\bar{B}$ pairs at the LHC or supposed to be produced at the Super-LHC. At the end, we conclude that the study of these asymmetries for $\bar{B} \rightarrow \bar{K}_0^*(1430)\ell^+\ell^-$ and $\bar{B} \rightarrow \bar{K}\ell^+\ell^-$ processes are very effective tools for establishing new physics in the future B-physics experiments.

Packs numbers: 12.60.-i, 13.30.-a, 14.20.Mr

I. INTRODUCTION

The flavor changing neutral current (FCNC) processes induced by $b \rightarrow s\ell^+\ell^-$ ($\ell = e, \mu, \tau$) transitions provide an important testing ground to test the standard model (SM) at one loop level, since they are forbidden in SM at tree level [10, 11]. Therefore these decays are very sensitive to the physics beyond the SM via the influence of new particles in the loops.

Although the branching ratios of FCNC decays are small in the SM, interesting results are yielded in developing experiments. The inclusive $b \rightarrow X_s\ell^+\ell^-$ decay is observed in BaBar [12] and Belle collaborations. These collaborations also measured exclusive modes $B \rightarrow K\ell^+\ell^-$ [13–15] and $B \rightarrow K^*\ell^+\ell^-$ [16]. These experimental results have high agreement with theoretical predictions [17–19].

There exists another group of rare decays induced by $b \rightarrow s$ transition, such as $B \rightarrow K_2^*(1430)\ell^+\ell^-$ and $B \rightarrow K_0^*(1430)\ell^+\ell^-$ in which B meson decays into a tensor or scalar meson, respectively. These decays are deeply investigated in SM in [20, 21] and the related transition form factors are formulated within the framework of light front quark model [21–23] and QCD sum rules method [24, 25], respectively. Lately these rare decays have been the matter of various physical discussions in the frame work of some new physics models, such as models including universal extra dimension [26], supersymmetry particles [27] and the fourth-generation fermions [28]. Generally, by studying the physical observables of these decay modes there would be a chance for testing SM or probing possible NP models. These physical quantities are for example the branching ratio, the forward-backward asymmetry, the lepton polarization asymmetry, the isospin asymmetry and etc.

The SM of electroweak interactions has been strictly tested over the past twenty years and shows an excellent compatibility with all collider data. The dynamics of electroweak symmetry breaking, however, is not exactly known. While the simplest possibility is the minimal Higgs mechanism which suggests a single scalar SU(2) doublet, many extensions of the SM predict a large Higgs sector to contain more scalars [29, 30].

Two conditions which tightly constrain the extensions of the SM Higgs sector are first the value of rho parameter, $\rho \equiv M_W^2/M_Z^2 \cos^2 \theta_W \simeq 1$, where M_W (M_Z) is the W^\pm (Z) boson mass and θ_W is the weak mixing angle and second the absence of large flavor-changing neutral currents. The first of these conditions is spontaneously fulfilled by Higgs sectors that consists only SU(2) doublets (with the possibly additional singlets). The simplest such model that contains a charged Higgs boson is a two-Higgs-doublet model (2HDM). The second of these conditions is

* falahati@shirazu.ac.ir

spontaneously satisfied by models in which the masses of fermions are produced through couplings to exactly one Higgs doublet; this is known as natural flavor conservation and forbids the tree-level flavor-changing neutral Higgs interactions phenomena.

Imposing natural flavor conservation by considering an *ad hoc* discrete symmetry [31], there would be two different ways to couple the SM fermions to two Higgs doublets. The Type-I and -II 2HDMs which have been studied extensively in the literatures, are such models [30]. Without considering discrete symmetry a more general form of 2HDM, namely, model III has been obtained which allows for the presence of FCNC at tree level. Consistent with the low energy constraints, the FCNC's involving the first two generations are highly suppressed, and those involving the third generation is not as severely suppressed as the first two generations. Also, in such a model there exists rich induced CP-violating sources from a single CP phase of vacuum that is absent in the SM, model I and model II. In order to consider the flavor-conserving limit of the Type III, we suppose that the two Yukawa matrices for each fermion type to be diagonal in the same fermion mixing basis [32]. All three structures of 2HDM generally contain two scalar Higgs bosons h^0, H^0 , one pseudoscalar Higgs boson A^0 and one charged Higgs boson H^\pm .

The aim of the present paper is to perform a comprehensive study regarding the polarized and unpolarized forward-backward asymmetries of $\bar{B} \rightarrow \bar{K}_0^*(1430)\ell^+\ell^-$ decays in the SM and the Model III of 2HDM. Also, we consider the influences of such models on the same asymmetries of $\bar{B} \rightarrow \bar{K}\ell^+\ell^-$ decays. In such a way, we study the sensitivity of results to the scalar property or the pseudo-scalar property of produced mesons.

The paper is organized as follows. In Section II, starting from the 2HDM form of four-Fermi interactions we derive the expressions for the matrix elements of B to a scalar meson and B to a pseudo-scalar meson, here $\bar{B} \rightarrow \bar{K}_0^*(1430)\ell^+\ell^-$ and $\bar{B} \rightarrow \bar{K}\ell^+\ell^-$, respectively. Then the general expressions for the polarized and unpolarized lepton pair forward-backward asymmetries have been extracted out. The sensitivity of these polarizations and the corresponding averages to the model III 2HDM parameters have been numerically analyzed in Section III. In the final section a brief summary of our results is presented.

II. ANALYTIC FORMULAS

A. The Effective Hamiltonian for $\bar{B} \rightarrow \bar{K}\ell^+\ell^-$ and $\bar{B} \rightarrow \bar{K}_0^*(1430)\ell^+\ell^-$ transitions in SM and 2HDM

The exclusive decays $\bar{B} \rightarrow \bar{K}\ell^+\ell^-$ and $\bar{B} \rightarrow \bar{K}_0^*(1430)\ell^+\ell^-$ are described at quark level by $b \rightarrow s\ell^+\ell^-$ transition. The effective Hamiltonian, that is used to describe the $b \rightarrow s\ell^+\ell^-$ transition in 2HDM models is:

$$\mathcal{H}_{eff}(b \rightarrow s\ell^+\ell^-) = -\frac{4G_F}{\sqrt{2}}V_{tb}V_{ts}^* \left\{ \sum_{i=1}^{10} C_i(\mu)O_i(\mu) + \sum_{i=1}^{10} C_{Q_i}(\mu)Q_i(\mu) \right\}, \quad (1)$$

where the first part is related to the effective Hamiltonian in the SM such that the respective Wilson coefficients get extra terms due to the presence of charged Higgs bosons. The second part which includes new operators is extracted from contributing the massive neutral Higgs bosons to this decay. All operators as well as the related Wilson coefficients are given in [33–35]. Now, using the above effective Hamiltonian, the one-loop matrix elements of $b \rightarrow s\ell^+\ell^-$ can be given as:

$$\begin{aligned} \mathcal{M} &= \langle s\ell^+\ell^- | \mathcal{H}_{eff} | b \rangle \\ &= -\frac{G_F \alpha}{2\sqrt{2}\pi} V_{tb} V_{ts}^* \left\{ \tilde{C}_9^{\text{eff}} \bar{s} \gamma_\mu (1 - \gamma_5) b \bar{\ell} \gamma^\mu \ell + \tilde{C}_{10} \bar{s} \gamma_\mu (1 - \gamma_5) b \bar{\ell} \gamma^\mu \gamma_5 \ell \right. \\ &\quad - 2C_7^{\text{eff}} \frac{m_b}{q^2} \bar{s} i \sigma_{\mu\nu} q^\nu (1 + \gamma_5) b \bar{\ell} \gamma^\mu \ell - 2C_7^{\text{eff}} \frac{m_s}{q^2} \bar{s} i \sigma_{\mu\nu} q^\nu (1 - \gamma_5) b \bar{\ell} \gamma^\mu \ell \\ &\quad \left. + C_{Q_1} \bar{s} (1 + \gamma_5) b \bar{\ell} \ell + C_{Q_2} \bar{s} (1 + \gamma_5) b \bar{\ell} \gamma_5 \ell \right\}. \end{aligned} \quad (2)$$

The evolution of Wilson coefficients $C_7^{\text{eff}}, \tilde{C}_9^{\text{eff}}, \tilde{C}_{10}$ from the higher scale $\mu = m_W$ to the lower scale $\mu = m_b$ is described by the renormalization group equation. These coefficients at the scale $\mu = m_b$ are calculated in [33–35] and C_{Q_1} and C_{Q_2} at the same scale to leading order are

calculated in [35]. It should be noted that the coefficient $\tilde{C}_9^{\text{eff}}(\mu)$ can be decomposed into the following three parts:

$$\tilde{C}_9^{\text{eff}}(\mu) = \tilde{C}_9(\mu) + Y_{SD}(\hat{m}_c, \hat{s}) + Y_{LD}(\hat{m}_c, \hat{s}), \quad (3)$$

where the parameters \hat{m}_c and \hat{s} are defined as $\hat{m}_c = m_c/m_b$, $\hat{s} = q^2/m_b^2$. $Y_{SD}(\hat{m}_c, \hat{s})$ describes the short-distance contributions from four-quark operators far away from the $c\bar{c}$ resonance regions, which can be calculated reliably in the perturbative theory. The function $Y_{SD}(\hat{m}_c, \hat{s})$ is given by:

$$\begin{aligned} Y_{SD} = & g(\hat{m}_c, \hat{s})(3C_1 + C_2 + 3C_3 + C_4 + 3C_5 + C_6) \\ & - \frac{1}{2}g(1, \hat{s})(4C_3 + 4C_4 + 3C_5 + C_6) \\ & - \frac{1}{2}g(0, \hat{s})(C_3 + 3C_4) + \frac{2}{9}(3C_3 + C_4 + 3C_5 + C_6), \end{aligned} \quad (4)$$

where the explicit expressions for the g functions can be found in [33]. The long-distance contributions $Y_{LD}(\hat{m}_c, \hat{s})$ from four-quark operators near the $c\bar{c}$ resonance cannot be calculated from first principles of QCD and are usually parameterized in the form of a phenomenological Breit-Wigner formula making use of the vacuum saturation approximation and quark-hadron duality. The function $Y_{LD}(\hat{m}_c, \hat{s})$ is given by [7, 8]:

$$Y_{LD} = \frac{3\pi}{\alpha^2} C^{(0)} \sum_{V_i=\psi, \psi', \dots} k_i \frac{\Gamma(V_i \rightarrow \ell^+ \ell^-) m_{V_i}}{m_{V_i}^2 - q^2 - im_{V_i} \Gamma_{V_i}},$$

where α is the fine structure constant and $C^{(0)} = (3C_1 + C_2 + 3C_3 + C_4 + 3C_5 + C_6)$. The phenomenological parameters k_i for the $\bar{B} \rightarrow \bar{K} \ell^+ \ell^-$ decay can be fixed from $Br(\bar{B} \rightarrow J/\psi \bar{K} \rightarrow \bar{K} \ell^+ \ell^-) = Br(\bar{B} \rightarrow J/\psi \bar{K}) Br(J/\psi \rightarrow \ell^+ \ell^-)$. For the lowest resonances ψ and ψ' we will use $k_1 = 2.70$ and $k_2 = 3.51$, respectively [24]. Also, for the $\bar{B} \rightarrow \bar{K}_0^*(1430) \ell^+ \ell^-$ decay such parameters can be determined by $Br(\bar{B} \rightarrow J/\psi \bar{K}_0^*(1430) \rightarrow \bar{K}_0^*(1430) \ell^+ \ell^-) = Br(\bar{B} \rightarrow J/\psi \bar{K}_0^*(1430)) Br(J/\psi \rightarrow \ell^+ \ell^-)$. However, since the branching ratio of $\bar{B} \rightarrow J/\psi \bar{K}_0^*(1430)$ decay has not been measured yet, we assume that the values of k_i are in the order of one. Therefore, we use $k_1 = 1$ and $k_2 = 1$ in the following numerical calculations [8].

B. Form factors for $\bar{B} \rightarrow \bar{K} \ell^+ \ell^-$ transition

The exclusive $\bar{B} \rightarrow \bar{K} \ell^+ \ell^-$ decay is described in terms of the matrix elements of the quark operators in Eq. (2) over meson states, which can be parameterized in terms of the form factors. The needed matrix elements for the calculation of $\bar{B} \rightarrow \bar{K} \ell^+ \ell^-$ decay are:

$$\begin{aligned} & \langle \bar{K} | \bar{s} \gamma_\mu (1 - \gamma_5) b | \bar{B} \rangle, \\ & \langle \bar{K} | \bar{s} i \sigma_{\mu\nu} q^\nu (1 \pm \gamma_5) b | \bar{B} \rangle, \\ & \langle \bar{K} | \bar{s} (1 + \gamma_5) b | \bar{B} \rangle, \end{aligned} \quad (5)$$

which can be obtained as follows:

$$\langle \bar{K}(p_K) | \bar{s} \gamma_\mu (1 \pm \gamma_5) b | \bar{B}(p_B) \rangle = [f_+(q^2)(p_B + p_K)_\mu + f_-(q^2)q_\mu], \quad (6)$$

$$= f_+(q^2) \left[(p_B + p_K)_\mu - \frac{(m_B^2 - m_K^2)}{q^2} q_\mu \right] + \frac{(m_B^2 - m_K^2)}{q^2} f_0(q^2) q_\mu,$$

$$\langle \bar{K}(p_K) | \bar{s} i \sigma_{\mu\nu} q^\nu (1 \pm \gamma_5) b | \bar{B}(p_B) \rangle = \frac{-f_T(q^2)}{m_B + m_K} [(p_B + p_K)_\mu q^2 - (m_B^2 - m_K^2) q_\mu], \quad (7)$$

where $q = p_B - p_K$ is the momentum transfer. In deriving Eq. (6) we have used the relationship

$$f_-(q^2) = \frac{(m_B^2 - m_K^2)}{q^2} [f_0(q^2) - f_+(q^2)]. \quad (8)$$

TABLE I: Form factors for $\bar{B} \rightarrow \bar{K}$ transition obtained in the LCQSR calculation are fitted to the 3-parameter form.

	F	$F(0)$	a_F	b_F
$f_+^{\bar{B} \rightarrow \bar{K}}$	0.341 ± 0.051	1.410	0.406	
$f_0^{\bar{B} \rightarrow \bar{K}}$	0.341 ± 0.051	0.410	-0.361	

Now, multiplying both sides of Eq. (6) with q^μ and using the equation of motion, the expression in terms of form factors for $\langle \bar{K} | \bar{s}(1 \pm \gamma_5)b | \bar{B} \rangle$ is calculated as:

$$\langle \bar{K}(p_K) | \bar{s}(1 \pm \gamma_5)b | \bar{B}(p_B) \rangle = \langle \bar{K}(p_K) | \bar{s}b | \bar{B}(p_B) \rangle = \frac{1}{m_b - m_s} [f_+(q^2)(p_B + p_K) \cdot q + f_-(q^2)q^2], \quad (9)$$

$$= \frac{f_0(q^2)}{m_b - m_s} (m_B^2 - m_K^2) \quad (10)$$

$$\langle \bar{K}(p_K) | \bar{s}\gamma_5 b | \bar{B}(p_B) \rangle = 0.$$

For the form factors we have used the light cone QCD sum rules results [36] in which the q^2 dependence of the semileptonic form factors, f_0 and f_+ , is given by

$$F(q^2) = \frac{F(0)}{1 - a_F(q^2/m_B^2) + b_F(q^2/m_B^2)^2}, \quad (11)$$

where the values of parameters $F(0)$, a_F and b_F for the $\bar{B} \rightarrow \bar{K} \ell^+ \ell^-$ decay are listed in table I. Also, the q^2 dependence of the penguin form factor, f_T , is obtained by

$$\frac{f_T(q^2)}{m_B + m_K} = \frac{1}{m_b} \left[\left(1 + \frac{m_b^2 - q^2}{q^2}\right) f_+ - \frac{m_b^2 - q^2}{q^2} f_0 \right]. \quad (12)$$

C. Form factors for $\bar{B} \rightarrow \bar{K}_0^*(1430) \ell^+ \ell^-$ transition

Like the exclusive $\bar{B} \rightarrow \bar{K} \ell^+ \ell^-$ decay, the $\bar{B} \rightarrow \bar{K}_0^*(1430) \ell^+ \ell^-$ transition is expressed by the matrix elements appeared in Eq. (5) except K is replaced by $K_0^*(1430)$. These physical objects could be parameterized as:

$$\langle \bar{K}_0^*(1430)(p_{K_0^*}) | \bar{s}\gamma_\mu(1 \pm \gamma_5)b | \bar{B}(p_B) \rangle = \pm [f_+(q^2)(p_B + p_{K_0^*})_\mu + f_-(q^2)q_\mu], \quad (13)$$

$$\langle \bar{K}_0^*(1430)(p_{K_0^*}) | \bar{s}i\sigma_{\mu\nu}q^\nu(1 \pm \gamma_5)b | \bar{B}(p_B) \rangle = \frac{\pm f_T(q^2)}{m_B + m_{K_0^*}} [(p_B + p_{K_0^*})_\mu q^2 - (m_B^2 - m_{K_0^*}^2)q_\mu], \quad (14)$$

$$\begin{aligned} \langle \bar{K}_0^*(1430)(p_{K_0^*}) | \bar{s}(1 \pm \gamma_5)b | \bar{B}(p_B) \rangle &= \pm \langle \bar{K}_0^*(1430)(p_{K_0^*}) | \bar{s}\gamma_5 b | \bar{B}(p_B) \rangle = \mp \frac{1}{m_b + m_s} [f_+(q^2)(p_B + p_{K_0^*}) \cdot q + f_-(q^2)q^2] \\ &= \mp \frac{f_0(q^2)}{m_b + m_s} (m_B^2 - m_{K_0^*}^2), \end{aligned} \quad (15)$$

$$\langle \bar{K}_0^*(1430)(p_{K_0^*}) | \bar{s}b | \bar{B}(p_B) \rangle = 0. \quad (16)$$

where $q = p_B - p_{K_0^*}$ and the function $f_0(q^2)$ has been extracted from the Eq. (8). For the form factors we have used the results of three-point QCD sum rules method [24] in which the q^2 dependence of the all form factors is given by

$$F(q^2) = \frac{F(0)}{1 - a_F(q^2/m_B^2) + b_F(q^2/m_B^2)^2}, \quad (17)$$

where the values of parameters $F(0)$, a_F and b_F for the $\bar{B} \rightarrow \bar{K}_0^*(1430) \ell^+ \ell^-$ decay are exhibited in table II.

TABLE II: Form factors for $\bar{B} \rightarrow \bar{K}_0^*(1430)$ transition obtained within three-point QCD sum rules are fitted to the 3-parameter form.

F	$F(0)$	a_F	b_F
$f_+^{\bar{B} \rightarrow \bar{K}_0^*}$	0.31 ± 0.08	0.81	-0.21
$f_-^{\bar{B} \rightarrow \bar{K}_0^*}$	-0.31 ± 0.07	0.80	-0.36
$f_T^{\bar{B} \rightarrow \bar{K}_0^*}$	-0.26 ± 0.07	0.41	-0.32

D. The differential decay rates and forward-backward asymmetries of $\bar{B} \rightarrow \bar{K}_0^*(1430)\ell^+\ell^-$

Making use of Eq.(2) and the definitions of form factors, the matrix element of the $\bar{B} \rightarrow \bar{K}_0^*(1430)\ell^+\ell^-$ decay can be written as follows:

$$\mathcal{M} = \frac{G_F \alpha_{\text{em}}}{4\sqrt{2}\pi} V_{ts}^* V_{tb} m_B \left\{ [\mathcal{A}(p_B + p_{K_0^*} + \mathcal{B}q_\mu)_\mu] \bar{\ell} \gamma^\mu \ell + [\mathcal{C}(p_B + p_{K_0^*} + \mathcal{D}q_\mu)_\mu] \bar{\ell} \gamma^\mu \gamma_5 \ell + [\mathcal{Q}] \bar{\ell} \ell + [\mathcal{N}] \bar{\ell} \gamma_5 \ell \right\}, \quad (18)$$

where the auxiliary functions $\mathcal{A}, \dots, \mathcal{Q}$ are listed in the following:

$$\mathcal{A} = -2\tilde{C}_9^{\text{eff}} f_+(q^2) - 4(m_b + m_s) C_7^{\text{eff}} \frac{f_T(q^2)}{m_B + m_{K_0^*}}, \quad (19)$$

$$\mathcal{B} = -2\tilde{C}_9^{\text{eff}} f_-(q^2) + 4(m_b + m_s) C_7^{\text{eff}} \frac{f_T(q^2)}{(m_B + m_{K_0^*})q^2} (m_B^2 - m_{K_0^*}^2), \quad (20)$$

$$\mathcal{C} = -2\tilde{C}_{10} f_+(q^2), \quad (21)$$

$$\mathcal{D} = -2\tilde{C}_{10} f_-(q^2), \quad (22)$$

$$\mathcal{Q} = -2C_{Q_1} f_0(q^2) \frac{(m_B^2 - m_{K_0^*}^2)}{m_b + m_s}, \quad (23)$$

$$\mathcal{N} = -2C_{Q_2} f_0(q^2) \frac{(m_B^2 - m_{K_0^*}^2)}{m_b + m_s}, \quad (24)$$

with $q = p_B - p_{K_0^*} = p_{\ell^+} + p_{\ell^-}$.

The unpolarized differential decay rate for the $\bar{B} \rightarrow \bar{K}_0^*(1430)\ell^+\ell^-$ decay in the rest frame of B meson is given by:

$$\frac{d\Gamma(\bar{B} \rightarrow \bar{K}_0^* \ell^+ \ell^-)}{d\hat{s}} = -\frac{G_F^2 \alpha_{\text{em}}^2 m_B}{2^{14} \pi^5} |V_{tb} V_{ts}^*|^2 v \sqrt{\lambda} \Delta, \quad (25)$$

with

$$\begin{aligned} \Delta = & 16m_\ell m_B^2 (1 - \hat{r}_{K_0^*}) \text{Re}[\mathcal{C} \mathcal{N}^*] + 4\hat{s} m_B^2 v^2 |\mathcal{Q}|^2 + 16\hat{s} m_\ell^2 m_B^2 |\mathcal{D}|^2 + 32m_\ell^2 m_B^2 (1 - \hat{r}_{K_0^*}) \text{Re}[\mathcal{C} \mathcal{D}^*] \\ & + 16\hat{s} m_\ell m_B^2 \text{Re}[\mathcal{D} \mathcal{N}^*] + 2\hat{s} m_B^2 |\mathcal{N}|^2 + \frac{4}{3} m_B^4 \lambda (3 - v^2) |\mathcal{A}|^2 \\ & + \frac{4}{3} m_B^4 |\mathcal{C}|^2 \{2\lambda - (1 - v^2)(2\lambda - 3(1 - \hat{r}_{K_0^*})^2)\}, \end{aligned} \quad (26)$$

where $v = \sqrt{1 - 4m_\ell^2/q^2}$, $\hat{s} = q^2/m_B^2$, $\hat{r}_{K_0^*} = m_{K_0^*}^2/m_B^2$ and $\lambda = 1 + \hat{r}_{K_0^*}^2 + \hat{s}^2 - 2\hat{r}_{K_0^*}(1 + \hat{s})$.

The unpolarized and normalized differential forward-backward asymmetry of the $\bar{B} \rightarrow \bar{K}_0^*(1430)\ell^+\ell^-$ decay in the center of mass frame of leptons is defined by:

$$\mathcal{A}_{FB} = \frac{\int_0^1 \frac{d^2\Gamma}{d\hat{s}dz} - \int_{-1}^0 \frac{d^2\Gamma}{d\hat{s}dz}}{\int_0^1 \frac{d^2\Gamma}{d\hat{s}dz} + \int_{-1}^0 \frac{d^2\Gamma}{d\hat{s}dz}}, \quad (27)$$

where $z = \cos \theta$ and θ is the angle between three momenta of the B meson and the negatively charged lepton (ℓ^-) in the CM (center of mass) frame of leptons.

Using the above-mentioned definition, the result can be written as follows:

$$\mathcal{A}_{FB}(\hat{s}) = \frac{8m_B^2 m_\ell v \sqrt{\lambda}}{\Delta} \text{Re}[\mathcal{A} \mathcal{Q}^*]. \quad (28)$$

Having obtained the unpolarized and normalized differential forward-backward asymmetry, let us now consider the normalized differential forward-backward asymmetries associated with the polarized leptons. For this purpose, we first define the following orthogonal unit vectors $s_i^{\pm\mu}$ in the rest frame of ℓ^\pm , where $i = L, N$ or T are the abbreviations of the longitudinal, normal and transversal spin projections, respectively:

$$\begin{aligned} s_L^{-\mu} &= (0, \vec{e}_L^-) = \left(0, \frac{\vec{p}_{\ell^-}}{|\vec{p}_{\ell^-}|}\right), \\ s_N^{-\mu} &= (0, \vec{e}_N^-) = \left(0, \frac{\vec{p}_{K_0^*} \times \vec{p}_{\ell^-}}{|\vec{p}_{K_0^*} \times \vec{p}_{\ell^-}|}\right), \\ s_T^{-\mu} &= (0, \vec{e}_T^-) = (0, \vec{e}_N^- \times \vec{e}_L^-), \\ s_L^{+\mu} &= (0, \vec{e}_L^+) = \left(0, \frac{\vec{p}_{\ell^+}}{|\vec{p}_{\ell^+}|}\right), \\ s_N^{+\mu} &= (0, \vec{e}_N^+) = \left(0, \frac{\vec{p}_{K_0^*} \times \vec{p}_{\ell^+}}{|\vec{p}_{K_0^*} \times \vec{p}_{\ell^+}|}\right), \\ s_T^{+\mu} &= (0, \vec{e}_T^+) = (0, \vec{e}_N^+ \times \vec{e}_L^+), \end{aligned} \quad (29)$$

where \vec{p}_{ℓ^\mp} and $\vec{p}_{K_0^*}$ are in the CM frame of $\ell^- \ell^+$ system, respectively. Lorentz transformation is used to boost the components of the lepton polarization to the CM frame of the lepton pair as:

$$\begin{aligned} (s_L^{\mp\mu})_{CM} &= \left(\frac{|\vec{p}_{\ell^\mp}|}{m_\ell}, \frac{E_\ell \vec{p}_{\ell^\mp}}{m_\ell |\vec{p}_{\ell^\mp}|}\right), \\ (s_N^{\mp\mu})_{CM} &= (s_N^{\mp\mu})_{RF}, \\ (s_T^{\mp\mu})_{CM} &= (s_T^{\mp\mu})_{RF}, \end{aligned} \quad (30)$$

where RF refers to the rest frame of the corresponding lepton as well as $\vec{p}_{\ell^+} = -\vec{p}_{\ell^-}$ and E_ℓ and m_ℓ are the energy and mass of leptons in the CM frame, respectively.

The polarized and normalized differential forward-backward asymmetry can be defined as:

$$\begin{aligned} \mathcal{A}_{FB}^{ij}(\hat{s}) &= \left(\frac{d\Gamma(\hat{s})}{d\hat{s}}\right)^{-1} \left\{ \int_0^1 dz - \int_{-1}^0 dz \right\} \left\{ \left[\frac{d^2\Gamma(\hat{s}, \vec{s}^- = \vec{i}, \vec{s}^+ = \vec{j})}{d\hat{s}dz} - \frac{d^2\Gamma(\hat{s}, \vec{s}^- = \vec{i}, \vec{s}^+ = -\vec{j})}{d\hat{s}dz} \right] \right. \\ &\quad \left. - \left[\frac{d^2\Gamma(\hat{s}, \vec{s}^- = -\vec{i}, \vec{s}^+ = \vec{j})}{d\hat{s}dz} - \frac{d^2\Gamma(\hat{s}, \vec{s}^- = -\vec{i}, \vec{s}^+ = -\vec{j})}{d\hat{s}dz} \right] \right\} \\ &= \mathcal{A}_{FB}(\vec{s}^- = \vec{i}, \vec{s}^+ = \vec{j}) - \mathcal{A}_{FB}(\vec{s}^- = \vec{i}, \vec{s}^+ = -\vec{j}) - \mathcal{A}_{FB}(\vec{s}^- = -\vec{i}, \vec{s}^+ = \vec{j}) \\ &\quad + \mathcal{A}_{FB}(\vec{s}^- = -\vec{i}, \vec{s}^+ = -\vec{j}), \end{aligned} \quad (31)$$

where $\frac{d\Gamma(\hat{s})}{d\hat{s}}$ is calculated in the CM frame. Using these definitions for the double polarized FB asymmetries, the following explicit forms for \mathcal{A}_{FB}^{ij} 's are obtained:

$$\mathcal{A}_{FB}^{LL} = -\mathcal{A}_{FB}^{NN} = -\mathcal{A}_{FB}^{TT} = \mathcal{A}_{FB}, \quad (32)$$

$$\mathcal{A}_{FB}^{LN} = \frac{-16v\lambda m_\ell m_B^3}{3\sqrt{\hat{s}}\Delta} \text{Im}[\mathcal{A} \mathcal{C}^*], \quad (33)$$

$$\mathcal{A}_{FB}^{NL} = \mathcal{A}_{FB}^{LN}, \quad (34)$$

$$\mathcal{A}_{FB}^{LT} = \frac{-16\lambda m_\ell m_B^3}{3\sqrt{\hat{s}}\Delta} |\mathcal{A}|^2, \quad (35)$$

$$\mathcal{A}_{FB}^{TL} = \mathcal{A}_{FB}^{LT}, \quad (36)$$

$$\mathcal{A}_{FB}^{NT} = \frac{8m_B^2 m_\ell \sqrt{\lambda}}{\Delta} \text{Im} \left[-2 \frac{m_\ell}{\hat{s}} (\mathcal{A} \mathcal{C}^*) (1 - \hat{r}_{K_0^*}) - (\mathcal{A} \mathcal{N}^*) + 2m_\ell (\mathcal{D} \mathcal{A}^*) \right], \quad (37)$$

$$\mathcal{A}_{FB}^{TN} = -\mathcal{A}_{FB}^{NT}. \quad (38)$$

E. The differential decay rates and forward-backward asymmetries of $\bar{B} \rightarrow \bar{K} \ell^+ \ell^-$

Imposing $m_s = 0$ in the whole afore-mentioned expressions for $\bar{B} \rightarrow \bar{K}_0^*(1430) \ell^+ \ell^-$ and $\bar{B} \rightarrow \bar{K} \ell^+ \ell^-$, we could obtain the similar expressions for $\bar{B} \rightarrow \bar{K} \ell^+ \ell^-$ decay, such that all the above equations remain unchanged except the definitions of the auxiliary functions (Eqs.(19-24)). It is obvious from the matrix elements of the above-said decays, in order to obtain the auxiliary functions of the latter decay we should perform the following substitutions:

$$f_+^{K_0^*} \rightarrow -f_+^K, \quad f_-^{K_0^*} \rightarrow -f_-^K, \quad f_T^{K_0^*} \rightarrow -f_T^K. \quad (39)$$

III. NUMERICAL RESULTS AND DISCUSSION

In this section we shall focus on the concrete models such as SM and Model III of 2HDM. We study the effects of such models on the polarized and unpolarized forward-backward asymmetries and their averages for $\bar{B} \rightarrow \bar{K}_0^*(1430) \ell^+ \ell^-$ and $\bar{B} \rightarrow \bar{K} \ell^+ \ell^-$ decays. At the end, we compare the results of different decay modes to each other. The corresponding averages are defined by the following equation [9]:

$$\langle \mathcal{A}_{FB}^{ij} \rangle = \frac{\int_{4\hat{m}_\ell^2}^{(1-\sqrt{\hat{r}_M})^2} \mathcal{A}_{FB}^{ij} \frac{d\mathcal{B}}{d\hat{s}} d\hat{s}}{\int_{4\hat{m}_\ell^2}^{(1-\sqrt{\hat{r}_M})^2} \frac{d\mathcal{B}}{d\hat{s}} d\hat{s}}, \quad (40)$$

where the subscript M refers to $\bar{K}_0^*(1430)$ and \bar{K} mesons. The full kinematical interval of the dilepton invariant mass q^2 is $4m_\ell^2 \leq q^2 \leq (m_B - m_M)^2$ for which the long distance contributions (the charmonium resonances) can give substantial effects by considering the two low lying resonances J/ψ and ψ' , in the interval of $8 \text{ GeV}^2 \leq q^2 \leq 14 \text{ GeV}^2$. In order to decrease the hadronic uncertainties we use the kinematical region of q^2 for muon as [8]:

$$\text{I} \quad 4m_\ell^2 \leq q^2 \leq (m_{J\psi} - 0.02 \text{ GeV})^2,$$

$$\text{II} \quad (m_{J\psi} + 0.02 \text{ GeV})^2 \leq q^2 \leq (m_{\psi'} - 0.02 \text{ GeV})^2,$$

$$\text{III} \quad (m_{\psi'} + 0.02 \text{ GeV})^2 \leq q^2 \leq (m_B - m_M)^2,$$

and for tau as:

$$\text{I} \quad 4m_\ell^2 \leq q^2 \leq (m_{\psi'} - 0.02 \text{ GeV})^2,$$

$$\text{II} \quad (m_{\psi'} + 0.02 \text{ GeV})^2 \leq q^2 \leq (m_B - m_M)^2.$$

In Model III of 2HDM apart from the masses of Higgs bosons, two vertex parameters, λ_{tt} and λ_{bb} , are appeared in the calculations of the related Feynman diagrams. Since these coefficients can be complex, we can rewrite the following combination as:

$$\lambda_{tt} \lambda_{bb} = |\lambda_{tt} \lambda_{bb}| e^{i\theta}, \quad (41)$$

in which the range of variations for $|\lambda_{tt}|$, $|\lambda_{bb}|$ and the phase angle θ are given by the experimental limits of the electric dipole moments of neutron(NEDM), $B^0 - \bar{B}^0$ mixing, ρ_0 , R_b and $Br(b \rightarrow s\gamma)$ [30, 32, 37, 38]. The experimental bounds on NEDM and $Br(b \rightarrow s\gamma)$ as well as M_{H^\pm} which are obtained at LEP II constrain $\lambda_{tt}\lambda_{bb}$ to be closely equal to 1 and the phase angle θ to be between $60^\circ - 90^\circ$. The next restriction which comes from the experimental value of x_d parameter, corresponding to the $B^0 - \bar{B}^0$ mixing, controls $|\lambda_{tt}|$ to be less than 0.3. Also, the experimental value of parameter R_b which is defined as $R_b \equiv \frac{\Gamma(Z \rightarrow b\bar{b})}{\Gamma(Z \rightarrow \text{hadrons})}$ affects on the magnitude of $|\lambda_{bb}|$ in such away this coefficient could be around 50. Using these restrictions and taking $\theta = \pi/2$, we consider the following three typical parameter cases throughout the numerical analysis[32]:

$$\begin{aligned} \text{CaseA : } |\lambda_{tt}| &= 0.03; \quad |\lambda_{bb}| = 100, \\ \text{CaseB : } |\lambda_{tt}| &= 0.15; \quad |\lambda_{bb}| = 50, \\ \text{CaseC : } |\lambda_{tt}| &= 0.3; \quad |\lambda_{bb}| = 30. \end{aligned} \tag{42}$$

The other main input parameters are the form factors which are listed in tables I and II. In addition, in this study we have applied four sets of masses of Higgs bosons which are displayed in tableIII[32].

TABLE III: List of the values for the masses of the Higgs particles.

	m_{H^\pm}	m_{A^0}	m_{H^0}	m_{H^\pm}
mass set – 1	200Gev	125Gev	125Gev	160Gev
mass set – 2	160Gev	125Gev	125Gev	160Gev
mass set – 3	200Gev	125Gev	125Gev	125Gev
mass set – 4	160Gev	125Gev	125Gev	125Gev

We have shown our analysis for the dependency of \mathcal{A}_{FB}^{ij} 's and their averages on the parameters of Model III of 2HDM in a set of figures (1-12) and tables (IV-XI), respectively. Moreover, in these tables the theoretical and experimental uncertainties corresponding to the SM averages for $\bar{B} \rightarrow \bar{K}_0^*(1430)\ell^+\ell^-$ and $\bar{B} \rightarrow \bar{K}\ell^+\ell^-$ decays have been taken into account. It should also be mentioned finally that the theoretical uncertainties are extracted from the hadronic uncertainties related to the form factors and the experimental uncertainties originate from the mass of quarks and hadrons and Wolfenstein parameters. In the following analyses we have just talked about the asymmetries whose predictions are larger than 0.005 in 2HDM.

- **Analysis of \mathcal{A}_{FB} asymmetries for $\bar{B} \rightarrow \bar{K}_0^*\mu^+\mu^-$ and $\bar{B} \rightarrow \bar{K}\mu^+\mu^-$ decays:** As it is obvious from figure 1 however the predictions of \mathcal{A}_{FB} for $\bar{B} \rightarrow \bar{K}_0^*\mu^+\mu^-$ in cases B and C for all mass sets coincide with that of SM which is zero throughout the domain $4m_\mu^2 < q^2 < (m_B - m_{K_0^*})^2$, such coincidence is not generally seen in case A. In this case within the interval $m_{\psi'}^2 < q^2 < (m_B - m_{K_0^*})^2$ a larger discrepancy between the predictions of SM and 2HDM is observed compared with those predictions in the range $4m_\mu^2 < q^2 < m_{\psi'}^2$. Also it is understood from these plots that whenever the mass of H^\pm increases or the mass of H^0 decreases this asymmetry shows more sensitivity to the existence of new Higgs bosons in such a manner that the most deviation from the anticipation of SM happens in the mass set 3 of the afore-mentioned case and range which is around 0.017 occurring next to $q^2 = (m_B - m_{K_0^*})^2$. In contrast, the magnitudes of averages related to tables IV and V could not provide any signs for the presence of new Higgs bosons since those values are less than 0.005 in both SM and 2HDM. It is also explicit from figure 2 and tables VI and VII that there are the same discussions regarding $\bar{B} \rightarrow \bar{K}\mu^+\mu^-$ decay as those of $\bar{B} \rightarrow \bar{K}_0^*\mu^+\mu^-$ decay except that the dependency of \mathcal{A}_{FB} on q^2 for $\bar{B} \rightarrow \bar{K}_0^*\mu^+\mu^-$ decay indicates more sensitivity to the 2HDM parameters. For instance while the largest prediction of the former decay is about 0.017, that of the latter decay is around 0.015. Based on this, experimental study of this observable for the μ channel of $\bar{B} \rightarrow \bar{K}_0^*$ and $\bar{B} \rightarrow \bar{K}$ transitions can be suitable in looking for new Higgs bosons.
- **Analysis of \mathcal{A}_{FB}^{LN} asymmetries for $\bar{B} \rightarrow \bar{K}_0^*\mu^+\mu^-$ and $\bar{B} \rightarrow \bar{K}\mu^+\mu^-$ decays:** It is seen from figure 3 that for the $\bar{B} \rightarrow \bar{K}_0^*\mu^+\mu^-$ decay the predictions of both mass sets 1 and 3 and both mass sets 2 and 4 are separately the same and the deviation from the SM value in

mass sets 2 and 4 is more than that in mass sets 1 and 3. Therefore, while this asymmetry is insensitive to the variation of mass of H^0 , it is susceptible to the change of mass of H^\pm , here the reduction of mass of such boson. Also, the relevant plots show that this quantity is quite sensitive to the variation of the parameters λ_{tt} and λ_{bb} . For example, by enhancing the magnitude of $|\lambda_{tt}\lambda_{bb}|$ the deviation from the SM value is increased. By combining the above analyses it is understood that the most deviation from the SM prediction occurs in the case C of mass sets 2 and 4. Particularly at $q^2 = 4m_\mu^2$ in the afore-mentioned case and mass-sets, a deviation around 30 times of the SM expectation is seen. In addition, it is found out through the corresponding tables that the values of averages show the same dependencies as those of diagrams to the existence of new Higgs bosons so that the most distance between the SM prediction and that of 2HDM arises in the case C of mass sets 2 and 4 which is 16 times of the SM anticipation. It is also evident from figure 4 and tables VI and VII that there are the similar explanations concerning $\bar{B} \rightarrow \bar{K}\mu^+\mu^-$ decay to those of $\bar{B} \rightarrow \bar{K}_0^*\mu^+\mu^-$ decay except that two Higgs doublet scenario can flip the sign of \mathcal{A}_{FB}^{LN} compared to the SM expectation in the latter decay in all cases and mass sets. The maximum deviations relative to the SM predictions which are observed in the respective diagrams and tables take place in the case C of mass sets 2 and 4 which are closely -55 times of the SM prediction for the corresponding diagrams occurring at $q^2 = 4m_\mu^2$ and -7 times of the SM prediction for the related averages. Therefore, it seems that the measurements of \mathcal{A}_{FB}^{LN} and its average for each of decay modes and its sign for the latter decay mode could provide appropriate ways to discover new Higgs bosons.

- Analysis of \mathcal{A}_{FB}^{NT} asymmetries for $\bar{B} \rightarrow \bar{K}_0^*\mu^+\mu^-$ and $\bar{B} \rightarrow \bar{K}\mu^+\mu^-$ decays:** It is found out from figure 5 that whereas the predictions of 2HDM in the domain $4m_c^2 < q^2 < (m_B - m_{K_0^*})^2$ for all mass sets and cases conform to that of SM, such conformity does not happen in the range $4m_\mu^2 < q^2 < 4m_c^2$. In this range, by increasing $|\lambda_{tt}\lambda_{bb}|$ the difference between the SM and 2HDM predictions becomes greater. Also while this asymmetry is independent from the variation of mass of H^0 , it is entirely sensitive to the reduction of mass of H^\pm so that the predictions of mass set 1 resemble those of mass set 3 and the predictions of mass set 2 resemble those of mass set 4. The most deviation from the SM value arises in the case C of mass sets 2 and 4 which is 26 times of the SM anticipation, occurring at $q^2 = 4m_\mu^2$. Moreover it is deduced from tables IV and V that the interval between the average of SM and those of cases A and B is less than 0.005, so the SM and cases A and B predictions overlap with each other and those values could not be useful for finding new physics. However, the difference between the values of case C and that of SM is larger than those of the other cases such that equals with 0.005 and thus the average of this case for all mass sets could be suitable for discovering new Higgs bosons. In addition it is understood from figure 6 that there are the same behaviors for $\bar{B} \rightarrow \bar{K}\mu^+\mu^-$ as those for $\bar{B} \rightarrow \bar{K}_0^*\mu^+\mu^-$ except that a change in the sign of \mathcal{A}_{FB}^{NT} for the latter decay is seen such that the most deviation from the SM anticipation is -26 times of the SM prediction. Also it is seen from tables VI and VII that the distance between the average of SM and those of all cases is less than 0.005 and hence the average of these cases could not be helpful for finding new Higgs bosons. Based on the above explanations, the measurement of this asymmetry for the afore-mentioned decays only in the range $4m_\mu^2 < q^2 < 4m_c^2$ may be promising in looking for new Higgs bosons.
- Analysis of \mathcal{A}_{FB} asymmetries for $\bar{B} \rightarrow \bar{K}_0^*\tau^+\tau^-$ and $\bar{B} \rightarrow \bar{K}\tau^+\tau^-$ decays:** As it is obvious from figure 7 although the predictions of \mathcal{A}_{FB} over the domain $4m_\tau^2 < q^2 < (m_B - m_{K_0^*})^2$ for $\bar{B} \rightarrow \bar{K}_0^*\tau^+\tau^-$ in cases B and C of all mass sets correspond to that of SM which is zero, such correspondence is not generally seen in case A. Also it is understood from these plots that during enhancing the mass of H^\pm or reducing the mass of H^0 this asymmetry shows more dependency to the existence of new Higgs bosons so that the most deviations from the anticipation of SM arise in the mass set 3 of the afore-mentioned case. Asymmetries up to ± 0.12 are possible as compared to SM prediction which occur around $q^2 = m_\psi^2$. Moreover it is found out from tables VIII and IX that the sensitivity of averages to the masses of Higgs bosons and cases is like the corresponding plots such that only the averages of case A can give promising information about the existence of new Higgs bosons and the largest average for this asymmetry compared to SM prediction happens in the mass set 3 which is 0.083. As it clear from figure 8 and tables X and XI there are similar expressions for $\bar{B} \rightarrow \bar{K}\tau^+\tau^-$ to those for $\bar{B} \rightarrow \bar{K}_0^*\tau^+\tau^-$ except that the magnitudes of maximum deviations of each of decay modes in the relevant diagrams and tables are different from those of other decay. Asymmetries up to -0.14 and +0.18 are possible as compared to SM prediction which occur at $q^2 = m_\psi^2$ and $q^2 = 18\text{GeV}^2$, respectively. Therefore, study of this observable and its average in the experiments, for the τ channel of $\bar{B} \rightarrow \bar{K}_0^*$ and $\bar{B} \rightarrow \bar{K}$ transitions, can give inspiring facts about the existence of new Higgs bosons.

- Analysis of A_{FB}^{LN} asymmetries for $\bar{B} \rightarrow \bar{K}_0^* \tau^+ \tau^-$ and $\bar{B} \rightarrow \bar{K} \tau^+ \tau^-$ decays:** It is apparent from figure 9 that for the $\bar{B} \rightarrow \bar{K}_0^* \tau^+ \tau^-$ decay the predictions of mass set 1 resemble those of mass set 3 and the predictions of mass set 2 resemble those of mass set 4 and the deviation from the SM value in mass sets 2 and 4 is larger than that in mass sets 1 and 3. Therefore, while the magnitude of this asymmetry does not change by varying the mass of H^0 , it is quite sensitive to the reduction of mass of H^\pm . Also, it is explicit from the relevant plots that this asymmetry is quite sensitive to the changes of the parameters λ_{tt} and λ_{bb} . For example, during enhancing the magnitude of $|\lambda_{tt} \lambda_{bb}|$ the deviation from the SM value is increased. By adding up the above analyses it is understood that the most deviation from the SM prediction takes place in the case C of mass sets 2 and 4. Specially at $q^2 = m_{\psi'}^2$ in the afore-mentioned case and mass-sets, a deviation around 2.6 times of the SM expectation is observed. Besides, it is found out through the corresponding tables that except for the averages of case A, those of the other cases are not in the range of SM prediction and their dependencies to the new Higgs boson parameters are like those of diagrams. For example, the most distance between the SM prediction and that of 2HDM arises in the case C of mass sets 2 and 4 which is 2.5 times of the SM anticipation. It is also evident from figure 10 and tables VI and VII that there are the similar explanations concerning $\bar{B} \rightarrow \bar{K} \tau^+ \tau^-$ decay to those of $\bar{B} \rightarrow \bar{K}_0^* \tau^+ \tau^-$ decay except that in the latter decay two Higgs doublet scenario can flip the sign of \mathcal{A}_{FB}^{LN} compared to the SM expectation in cases B and C of all mass sets. The maximum deviations relative to the SM predictions which are observed in the respective diagrams and tables take place in the case C of mass sets 2 and 4 which are closely -1 times of the SM prediction for the corresponding diagrams occurring at $q^2 = m_{\psi'}^2$ and -1.2 times of the SM prediction for the related averages. Therefore, it seems that the measurement of \mathcal{A}_{FB}^{LN} and its average for each of decay modes and its sign for the latter decay mode could provide a valuable tool in establishing new Higgs bosons.
- Analysis of A_{FB}^{NT} asymmetries for $\bar{B} \rightarrow \bar{K}_0^* \tau^+ \tau^-$ and $\bar{B} \rightarrow \bar{K} \tau^+ \tau^-$ decays:** It is evident through figure 11 and tables VIII and IX that for the former decay the predictions of mass set 1 resemble those of mass set 3 and likewise the predictions of mass set 2 resemble those of mass set 4. It is also revealed from the tables that the predictions of each of mass sets have not lain on the SM range. The most deviations compared to the SM predictions which are observed in the respective diagrams and tables take place in the case C of mass sets 2 and 4 which are closely 2.6 times of the SM prediction for the corresponding diagrams occurring at $q^2 = m_{\psi'}^2$ and 2.8 times of the SM prediction for the related averages. It is also obvious from figure 12 and tables X and XI that for the latter decay like the former decay the predictions of mass set 1 resemble those of mass set 3 and likewise the predictions of mass set 2 resemble those of mass set 4. In addition, while the predictions of \mathcal{A}_{FB}^{NT} over the domain $4m_\tau^2 < q^2 < (m_B - m_{K_0^*})^2$ in SM and case A are positive, those of cases B and C are completely negative. It is also explicit from the corresponding tables that the predictions of each of mass sets have not lain on the SM range. The most deviations compared to the SM predictions which are observed in the respective diagrams and tables take place in the case C of mass sets 2 and 4 which are closely -1.2 times of the SM prediction for the corresponding diagrams occurring at $q^2 = m_{\psi'}^2$ and -1.2 times of the SM prediction for the related averages. So, the measurements of A^{NT} and its average for each of decay modes and its sign for the latter decay mode can serve as good tests for discovering new Higgs bosons.

Finally, let us see briefly whether the lepton polarization asymmetries are testable or not. Experimentally, for measuring an asymmetry $\langle \mathcal{A}_{ij} \rangle$ of the decay with branching ratio \mathcal{B} at $n\sigma$ level, the required number of events (i.e., the number of $B\bar{B}$) is given by the formula

$$N = \frac{n^2}{\mathcal{B} s_1 s_2 \langle \mathcal{A}_{ij} \rangle^2},$$

where s_1 and s_2 are the efficiencies of the leptons. The values of the efficiencies of the τ -leptons differ from 50% to 90% for their various decay modes[39] and the error in τ -lepton polarization is approximately (10 – 15)% [40]. So, the error in measurements of the τ -lepton asymmetries is estimated to be about (20 – 30)%, and the error in obtaining the number of events is about 50%.

Based on the above expression for N , in order to detect the polarized and unpolarized forward backward asymmetries in the μ and τ channels at 3σ level, the lowest limit of required number of events are given by (the efficiency of τ -lepton is considered 0.5):

- for $\bar{B} \rightarrow \bar{K}_0^*(1430)\mu^+\mu^-$ decay

$$N \sim \begin{cases} 10^{12} & (\text{for } \langle \mathcal{A}_{FB} \rangle, \langle \mathcal{A}_{FB}^{LL} \rangle, \langle \mathcal{A}_{FB}^{TT} \rangle, \langle \mathcal{A}_{FB}^{NN} \rangle), \\ 10^{11} & (\text{for } \langle \mathcal{A}_{FB}^{LN} \rangle, \langle \mathcal{A}_{FB}^{NL} \rangle), \\ 10^9 & (\text{for } \langle \mathcal{A}_{FB}^{LT} \rangle, \langle \mathcal{A}_{FB}^{TL} \rangle), \\ 10^{12} & (\text{for } \langle \mathcal{A}_{FB}^{NT} \rangle, \langle \mathcal{A}_{FB}^{TN} \rangle), \end{cases}$$

- for $\bar{B} \rightarrow \bar{K}\mu^+\mu^-$ decay

$$N \sim \begin{cases} 10^{12} & (\text{for } \langle \mathcal{A}_{FB} \rangle, \langle \mathcal{A}_{FB}^{LL} \rangle, \langle \mathcal{A}_{FB}^{TT} \rangle, \langle \mathcal{A}_{FB}^{NN} \rangle), \\ 10^{10} & (\text{for } \langle \mathcal{A}_{FB}^{LN} \rangle, \langle \mathcal{A}_{FB}^{NL} \rangle), \\ 10^9 & (\text{for } \langle \mathcal{A}_{FB}^{LT} \rangle, \langle \mathcal{A}_{FB}^{TL} \rangle), \\ 10^{11} & (\text{for } \langle \mathcal{A}_{FB}^{NT} \rangle, \langle \mathcal{A}_{FB}^{TN} \rangle), \end{cases}$$

- for $\bar{B} \rightarrow \bar{K}_0^*(1430)\tau^+\tau^-$ decay

$$N \sim \begin{cases} 10^{12} & (\text{for } \langle \mathcal{A}_{FB} \rangle, \langle \mathcal{A}_{FB}^{LL} \rangle, \langle \mathcal{A}_{FB}^{TT} \rangle, \langle \mathcal{A}_{FB}^{NN} \rangle), \\ 10^{14} & (\text{for } \langle \mathcal{A}_{FB}^{LN} \rangle, \langle \mathcal{A}_{FB}^{NL} \rangle), \\ 10^{11} & (\text{for } \langle \mathcal{A}_{FB}^{LT} \rangle, \langle \mathcal{A}_{FB}^{TL} \rangle), \\ 10^{12} & (\text{for } \langle \mathcal{A}_{FB}^{NT} \rangle, \langle \mathcal{A}_{FB}^{TN} \rangle), \end{cases}$$

- for $\bar{B} \rightarrow \bar{K}\tau^+\tau^-$ decay

$$N \sim \begin{cases} 10^9 & (\text{for } \langle \mathcal{A}_{FB} \rangle, \langle \mathcal{A}_{FB}^{LL} \rangle, \langle \mathcal{A}_{FB}^{TT} \rangle, \langle \mathcal{A}_{FB}^{NN} \rangle), \\ 10^{11} & (\text{for } \langle \mathcal{A}_{FB}^{LN} \rangle, \langle \mathcal{A}_{FB}^{NL} \rangle), \\ 10^9 & (\text{for } \langle \mathcal{A}_{FB}^{LT} \rangle, \langle \mathcal{A}_{FB}^{TL} \rangle), \\ 10^{10} & (\text{for } \langle \mathcal{A}_{FB}^{NT} \rangle, \langle \mathcal{A}_{FB}^{TN} \rangle). \end{cases}$$

IV. SUMMARY

In short, in this paper by taking into account the theoretical and experimental uncertainties in the SM we have presented a comprehensive analysis regarding the polarized and unpolarized forward backward asymmetries for $\bar{B} \rightarrow \bar{K}_0^*\ell^+\ell^-$ and $\bar{B} \rightarrow \bar{K}\ell^+\ell^-$ decays using Model III of 2HDM. At the same time we have compared the results of both decay modes to each other. Also, the minimum required number of events for measuring each asymmetry has been obtained and compared with the number produced at the LHC experiments, containing ATLAS, CMS and LHCb, ($\sim 10^{12}$ per year) or expected to be produced at the Super-LHC experiments (supposed to be $\sim 10^{13}$ per year). In conclusion, the following results have been obtained:

i) For μ channel, only in \mathcal{A}^{LN} and \mathcal{A}^{NT} some sensitivities to the pseudo-scalar property or scalar property of produced mesons have been observed. For example, while the sign of \mathcal{A}^{LN} for $\bar{B} \rightarrow \bar{K}_0^*$ and $\bar{B} \rightarrow \bar{K}$ transitions in SM is positive that sign can change with the existence of Higgs bosons only in $\bar{B} \rightarrow \bar{K}$ transition. Also, the sign of \mathcal{A}^{NT} for each decay mode is the opposite of that of the other decay mode. Since the effects of 2HDM generally on the q^2 dependency of \mathcal{A}_{FB} , \mathcal{A}^{LN} and \mathcal{A}^{NT} and the average of \mathcal{A}^{LN} could be large and the minimum required number of $B\bar{B}$ pairs for the measurement of those asymmetries at the LHC are smaller than 10^{12} , so experimental studies of all mentioned asymmetries for each of decay modes can be suitable for searching Model III of 2HDM.

ii) For τ channel, in \mathcal{A}_{FB} , \mathcal{A}^{LN} and \mathcal{A}^{NT} some sensitivities to the pseudo-scalar feature or scalar feature of products have been observed. For instance, while the 2HDM signs of \mathcal{A}^{LN} and \mathcal{A}^{NT} in $\bar{B} \rightarrow \bar{K}$ transition change compared to SM predictions which are positive for \mathcal{A}^{LN} and negative for \mathcal{A}^{NT} such signs remain unchanged compared to SM predictions in $\bar{B} \rightarrow \bar{K}_0^*$ decay. Also for the \mathcal{A}_{FB} of different decay modes the values of q^2 at which the most deviations from the SM predictions happen are not the same. Moreover although the effects of 2HDM generally on the q^2 dependency of \mathcal{A}_{FB} , \mathcal{A}^{LN} and \mathcal{A}^{NT} and their averages could be large the minimum required number of events

for detecting such asymmetries at the LHC or SLHC impose some limitations for the measurements of those asymmetries. According to the above discussion for exploring Model III of 2HDM only experimental study of \mathcal{A}_{FB} and \mathcal{A}^{NT} are useful.

Finally, it is worthwhile mentioning that although the muon polarization is measured for stationary muons, such experiments are very hard to perform in the near future. The tau polarization can be studied by investigating the decay products of tau. The measurement of tau polarization in this respect is easier than the polarization of muon.

V. ACKNOWLEDGMENT

The authors would like to thank V. Bashiry for his useful discussions. Support of Research Council of Shiraz University is gratefully acknowledged.

TABLE IV: The averaged unpolarized and polarized forward-backward asymmetries for $\overline{B} \rightarrow \overline{K}_0^*(1430) \mu^+ \mu^-$ in SM and 2HDM for the mass sets 1 and 2 of Higgs bosons and the three cases A ($\theta = \pi/2$, $|\lambda_{tt}| = 0.03$ and $|\lambda_{bb}| = 100$), B ($\theta = \pi/2$, $|\lambda_{tt}| = 0.15$ and $|\lambda_{bb}| = 50$) and C ($\theta = \pi/2$, $|\lambda_{tt}| = 0.3$ and $|\lambda_{bb}| = 30$). The errors shown for each asymmetry are due to the theoretical and experimental uncertainties. The first ones are related to the theoretical uncertainties and the second ones are due to experimental uncertainties. The theoretical uncertainties come from the hadronic uncertainties related to the form factors and the experimental uncertainties originate from the mass of quarks and hadrons and Wolfenstein parameters.

	SM	Case A (Set 1)	Case B (Set1)	Case C (Set1)	Case A (Set 2)	Case B (Set 2)	Case C (Set 2)
$\langle \mathcal{A}_{FB} \rangle$	$0.000^{+0.000+0.000}_{-0.000-0.000}$	+0.001	+0.000	+0.000	+0.001	+0.000	+0.000
$\langle \mathcal{A}_{FB}^{LN} \rangle$	$+0.001^{+0.000+0.000}_{-0.000-0.000}$	+0.006	+0.012	+0.014	+0.006	+0.014	+0.016
$\langle \mathcal{A}_{FB}^{LT} \rangle$	$-0.072^{+0.002+0.004}_{-0.002-0.003}$	-0.072	-0.073	-0.072	-0.072	-0.073	-0.073
$\langle \mathcal{A}_{FB}^{NT} \rangle$	$-0.000^{+0.000+0.000}_{-0.000-0.000}$	-0.002	-0.004	-0.005	-0.002	-0.004	-0.005

TABLE V: The same as TABLE IV but for the mass sets 3 and 4 of Higgs bosons.

	SM	Case A (Set 3)	Case B (Set3)	Case C (Set3)	Case A (Set 4)	Case B (Set 4)	Case C (Set 4)
$\langle \mathcal{A}_{FB} \rangle$	$0.000^{+0.000+0.000}_{-0.000-0.000}$	+0.003	+0.000	+0.000	+0.002	+0.000	+0.000
$\langle \mathcal{A}_{FB}^{LN} \rangle$	$+0.001^{+0.000+0.000}_{-0.000-0.000}$	+0.006	+0.012	+0.014	+0.006	+0.014	+0.016
$\langle \mathcal{A}_{FB}^{LT} \rangle$	$-0.072^{+0.002+0.004}_{-0.002-0.003}$	-0.071	-0.073	-0.072	-0.072	-0.073	-0.073
$\langle \mathcal{A}_{FB}^{NT} \rangle$	$-0.000^{+0.000+0.000}_{-0.000-0.000}$	-0.002	-0.004	-0.005	-0.002	-0.004	-0.005

TABLE VI: The same as TABLE IV but for the $\bar{B} \rightarrow \bar{K} \mu^+ \mu^-$.

SM	Case A (Set 1)	Case B (Set1)	Case C (Set1)	Case A (Set 2)	Case B (Set 2)	Case C (Set 2)
$\langle \mathcal{A}_{FB} \rangle$	$0.000^{+0.000+0.000}_{-0.000-0.000}$	+0.001	+0.000	+0.000	+0.001	+0.000
$\langle \mathcal{A}_{FB}^{LN} \rangle$	$+0.002^{+0.000+0.000}_{-0.000-0.000}$	-0.003	-0.009	-0.011	-0.003	-0.011
$\langle \mathcal{A}_{FB}^{LT} \rangle$	$-0.051^{+0.018+0.000}_{-0.022-0.000}$	-0.051	-0.052	-0.052	-0.051	-0.052
$\langle \mathcal{A}_{FB}^{NT} \rangle$	$-0.000^{+0.000+0.000}_{-0.000-0.000}$	+0.000	+0.003	+0.003	+0.001	+0.003

TABLE VII: The same as TABLE VI except for the mass sets 3 and 4 of Higgs bosons.

SM	Case A (Set 3)	Case B (Set3)	Case C (Set3)	Case A (Set 4)	Case B (Set 4)	Case C (Set 4)
$\langle \mathcal{A}_{FB} \rangle$	$0.000^{+0.000+0.000}_{-0.000-0.000}$	+0.002	+0.000	+0.000	+0.002	+0.000
$\langle \mathcal{A}_{FB}^{LN} \rangle$	$+0.002^{+0.000+0.000}_{-0.000-0.000}$	-0.003	-0.009	-0.011	-0.003	-0.011
$\langle \mathcal{A}_{FB}^{LT} \rangle$	$-0.051^{+0.018+0.000}_{-0.022-0.000}$	-0.051	-0.052	-0.052	-0.051	-0.052
$\langle \mathcal{A}_{FB}^{NT} \rangle$	$-0.000^{+0.000+0.000}_{-0.000-0.000}$	+0.000	+0.003	+0.003	+0.001	+0.003

-
- [1] ATLAS Collaboration, "Observation of a new particle in the search for the Standard Model Higgs boson with the ATLAS detector at the LHC", Phys. Lett. **B 716**, 1 (2012).
- [2] CMS Collaboration, "Observation of a new boson at a mass of 125 GeV with the CMS experiment at the LHC", Phys. Lett. **B 716**, 30 (2012).
- [3] CMS Collaboration, "Observation of a new boson with mass near 125 GeV in pp collisions at $\sqrt{s} = 7$ and 8 TeV", JHEP **06**, 081 (2013).
- [4] T. M. Aliev and M. Savci, Phys. Rev. **D 60**, 014005 (1999).
- [5] M. Kobayashi and M. Maskawa, Prog. Theor. phys. **49**, 652 (1973).
- [6] T. P. Cheng and M. Sher, Phys. Rev. **D 35**, 3484 (1987); **D 44**, 1461 (1991).
- [7] F. Kruger. and L.M. Sehgal, Phys.Lett. **B 380**, 199 (1996).
- [8] V. Bashiry M. Bayar and K. Azizi, Mod. Phys. Lett. **A 26**, 901 (2011).
- [9] T. M. Aliev, M. K. Cakmak, A. Ozpineci and M. Savci, Phys.Rev. **D 64**, 055007 (2001).
- [10] G. Buchalla, A. J. Buras and M. E. Lautenbacher, Rev. Mod. Phys. **68**, 1125 (1996).
- [11] A. Ali, Int. J. Mod. Phys. **A 20**, 5080 (2005).
- [12] B. Aubert et. al, BaBar Collaboration, Phys. Rev. Lett. **93**, 081802 (2004).
- [13] M. I. Iwasaki et. al, BELLE Collaboration, Phys. Rev. **D 72**, 092005 (2005).
- [14] K. Abe et. al, BELLE Collaboration, Phys. Rev. Lett. **88**, 021801 (2002).
- [15] B. Aubert et. al, BaBar Collaboration, Phys. Rev. Lett. **91**, 221802 (2003).
- [16] A. Ishikawa et. al, BELLE Collaboration, Phys. Rev. Lett. **91**, 261601 (2003).
- [17] P. Colangelo, F. De Fazio, P. Santorelli and E. Scrimieri, Phys. Rev. **D 53**, 3672 (1996); Errata **D 57**, 3186 (1998); A. Ali, P. Ball, L. T. Handoko and G. Hiller, Phys. Rev. **D 61**, 074024 (2000); A. Ali, E. Lunghi, C. Greub and G. Hiller, Phys. Rev. **D 66**, 034002 (2002).
- [18] T. M. Aliev, H. Koru, A. Ozpineci, M. Savc, Phys. Lett. **B 400**, 194 (1997); T. M. Aliev, A. Ozpineci, M. Savc, Phys. Rev. **D 56**, 4260 (1997); D. Melikhov, N. Nikitin and S. Simula, Phys. Rev. **D 57**, 6814 (1998).

TABLE VIII: The same as TABLE IV except for $\bar{B} \rightarrow \bar{K}_0^*(1430)\tau^+\tau^-$.

SM	Case A	Case B	Case C	Case A	Case B	Case C
	(Set 1)	(Set1)	(Set1)	(Set 2)	(Set 2)	(Set 2)
$\langle \mathcal{A}_{FB} \rangle$	$0.000^{+0.000+0.000}_{-0.000-0.000}$	+0.045	+0.002	+0.000	+0.026	+0.001 +0.000
$\langle \mathcal{A}_{FB}^{LN} \rangle$	$+0.004^{+0.002+0.000}_{-0.004-0.000}$	+0.005	+0.008	+0.009	+0.005	+0.009 +0.010
$\langle \mathcal{A}_{FB}^{LT} \rangle$	$-0.176^{+0.080+0.008}_{-0.210-0.009}$	-0.160	-0.180	-0.178	-0.162	-0.181 -0.179
$\langle \mathcal{A}_{FB}^{NT} \rangle$	$-0.043^{+0.008+0.003}_{-0.007-0.002}$	-0.063	-0.099	-0.109	-0.067	-0.108 -0.120

TABLE IX: The same as TABLE VIII but for the mass sets 3 and 4 of Higgs bosons.

SM	Case A	Case B	Case C	Case A	Case B	Case C
	(Set 3)	(Set3)	(Set3)	(Set 4)	(Set 4)	(Set 4)
$\langle \mathcal{A}_{FB} \rangle$	$0.000^{+0.000+0.000}_{-0.000-0.000}$	+0.083	+0.004	+0.000	+0.056	+0.003 +0.000
$\langle \mathcal{A}_{FB}^{LN} \rangle$	$+0.004^{+0.002+0.000}_{-0.004-0.000}$	+0.005	+0.008	+0.009	+0.005	+0.009 +0.010
$\langle \mathcal{A}_{FB}^{LT} \rangle$	$-0.176^{+0.080+0.008}_{-0.210-0.009}$	-0.153	-0.180	-0.178	-0.158	-0.181 -0.179
$\langle \mathcal{A}_{FB}^{NT} \rangle$	$-0.043^{+0.008+0.003}_{-0.007-0.002}$	-0.060	-0.099	-0.109	-0.066	-0.108 -0.120

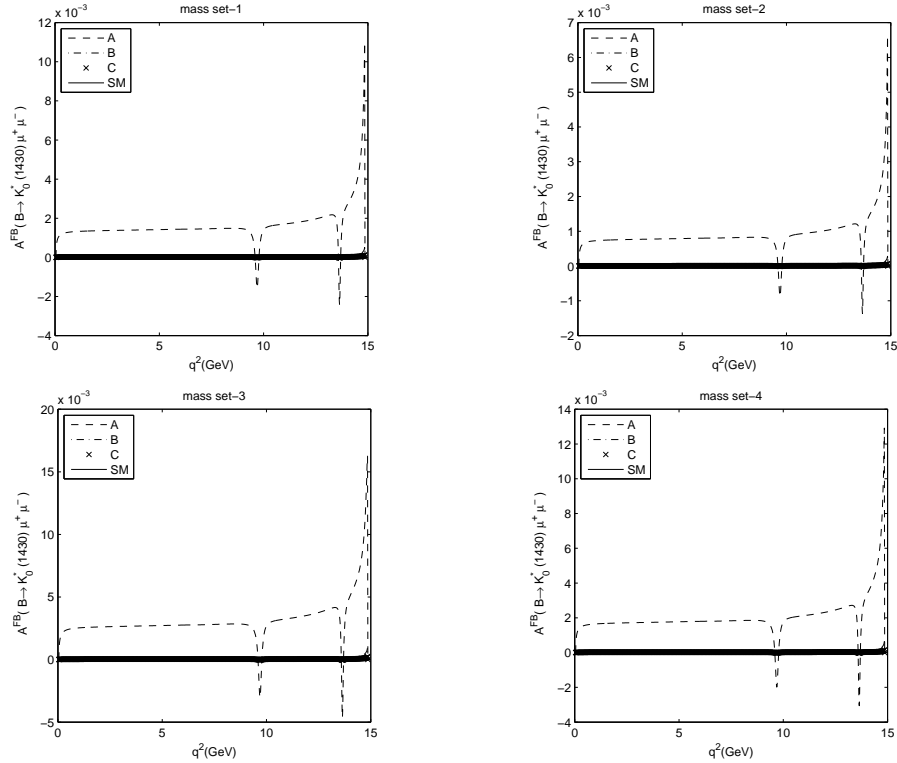
- [19] G. Burdman, Phys. Rev. **D 52**, 6400 (1995); J. L. Hewett and J. D. Walls, Phys. Rev. **D 55**, 5549 (1997); C. H. Chen and C. Q. Geng, Phys. Rev. **D 63**, 114025 (2001).
- [20] S. Rai Choudhury, A. S. Cornell, G. C. Joshi and B. H. J. McKellar, Phys. Rev. **D 74**, 054031 (2006).
- [21] H. Y. Cheng, C. K. Chua, and C. W. Huang, Phys. Rev. **D 69**, 074025 (2004).
- [22] H. Y. Cheng, C. K. Chua, Phys. Rev. **D 69**, 094007 (2004). [16]
- [23] C. H. Chen, C. Q. Geng, C. C. Lih and C. C. Liu, Phys. Rev. **D 75**, 074010 (2007).
- [24] T. M. Aliev, K. Azizi, M. Savci, Phys. Rev. **D 76**, 074017 (2007).
- [25] K. C. Yang, Phys. Lett. **B 695**, 444 (2011).
- [26] B. B. Sirvanli, K. Azizi, Y. Lpekoglu, JHEP **1101**, 069 (2011).
- [27] V. Bashiry, M. Bayar, K. Azizi, Mod. Phys. Lett. **A 26**, 901 (2011).
- [28] F. Falahati, R. Khosravi, Phys. Rev. **D 83** 015010 (2011).
- [29] C. Csaki, Mod. Phys. Lett. **A 11**, 599 (1996).
- [30] D. Atwood, L. Reina, and A. Soni, Phys. Rev. **D 55**, 3156 (1997).
- [31] S. Glashow and S. Weinberg, Phys. Rev. **D 15**, 1958 (1977).
- [32] D. Bowser-Chao, K. Cheung, and W. Y. Keung, Phys. Rev. **D 59**, 115006 (1999).
- [33] B. Grinstein, M. J. Savage and M. B. Wise, Nucl. Phys. **B 319**, 271 (1989).
- [34] A. J. Buras and M. Munz, Phys. Rev. **D 52**, 186 (1995).
- [35] Y. B. Dai, C. S. Huang, and H. W. Huang, Phys. Lett. **B 390**, 257 (1997).
- [36] P. Ball, JHEP **9809**, 005 (1998).
- [37] C. S. Huang and S. H. Zhu, Phys. Rev. **D 68**, 114020 (2003).
- [38] Y. B. Dai, C. S. Huang, J. T. Li and W. J. Li, Phys. Rev. **D 67**, 096007 (2003).
- [39] G. Abbiendi et al. (OPAL Collaboration), Phys. Lett. **B 492**, 23 (2000).
- [40] A. Rouge, Z. Phys. **C 48**, 75 (1990); in Proceedings of the Workshop on τ Lepton Physics, Orsay, France, 1990.

TABLE X: The same as TABLE VI except for $\bar{B} \rightarrow \bar{K} \tau^+ \tau^-$.

SM		Case A	Case B	Case C	Case A	Case B	Case C
		(Set 1)	(Set1)	(Set1)	(Set 2)	(Set 2)	(Set 2)
$\langle \mathcal{A}_{\text{FB}} \rangle$	$0.000^{+0.000+0.000}_{-0.000-0.000}$	+0.100	+0.005	+0.001	+0.059	+0.003	+0.000
$\langle \mathcal{A}_{\text{FB}}^{\text{LN}} \rangle$	$+0.014^{+0.004+0.000}_{-0.004-0.000}$	+0.004	-0.008	-0.013	+0.003	-0.012	-0.017
$\langle \mathcal{A}_{\text{FB}}^{\text{LT}} \rangle$	$-0.181^{+0.046+0.003}_{-0.053-0.003}$	-0.147	-0.178	-0.175	-0.156	-0.179	-0.176
$\langle \mathcal{A}_{\text{FB}}^{\text{NT}} \rangle$	$-0.054^{+0.003+0.000}_{-0.004-0.000}$	-0.017	+0.033	+0.049	-0.013	+0.048	+0.067

TABLE XI: The same as TABLE X but for the mass sets 3 and 4 of Higgs bosons.

SM		Case A	Case B	Case C	Case A	Case B	Case C
		(Set 3)	(Set3)	(Set3)	(Set 4)	(Set 4)	(Set 4)
$\langle \mathcal{A}_{\text{FB}} \rangle$	$0.000^{+0.000+0.000}_{-0.000-0.000}$	+0.155	+0.009	+0.002	+0.119	+0.006	+0.002
$\langle \mathcal{A}_{\text{FB}}^{\text{LN}} \rangle$	$+0.014^{+0.004+0.000}_{-0.004-0.000}$	+0.003	-0.008	-0.013	+0.003	-0.012	-0.017
$\langle \mathcal{A}_{\text{FB}}^{\text{LT}} \rangle$	$-0.181^{+0.046+0.003}_{-0.053-0.003}$	-0.118	-0.178	-0.175	-0.139	-0.178	-0.176
$\langle \mathcal{A}_{\text{FB}}^{\text{NT}} \rangle$	$-0.054^{+0.003+0.000}_{-0.004-0.000}$	-0.014	+0.033	+0.049	-0.011	+0.048	+0.067

FIG. 1: The dependence of the \mathcal{A}_{FB} polarization on q^2 and the three typical cases of 2HDM, i.e. cases A, B and C and SM for the μ channel of $\bar{B} \rightarrow \bar{K}_0^*$ transition for the mass sets 1, 2, 3 and 4.

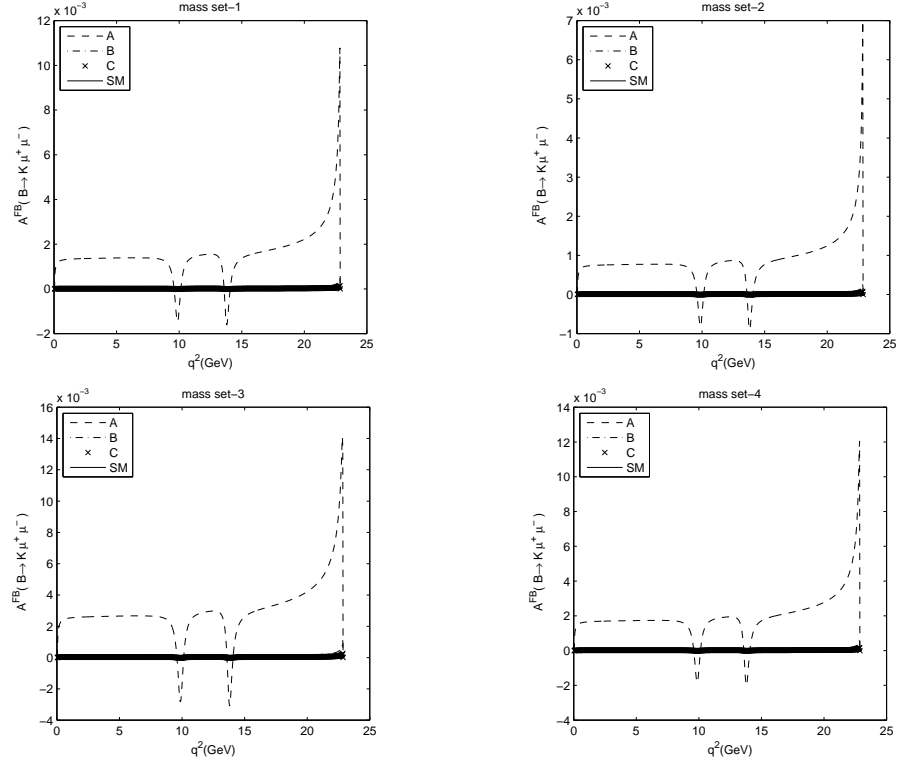


FIG. 2: The dependence of the \mathcal{A}_{FB} polarization on q^2 and the three typical cases of 2HDM, i.e. cases A, B and C and SM for the μ channel of $\overline{B} \rightarrow \overline{K}$ transition for the mass sets 1, 2, 3 and 4.

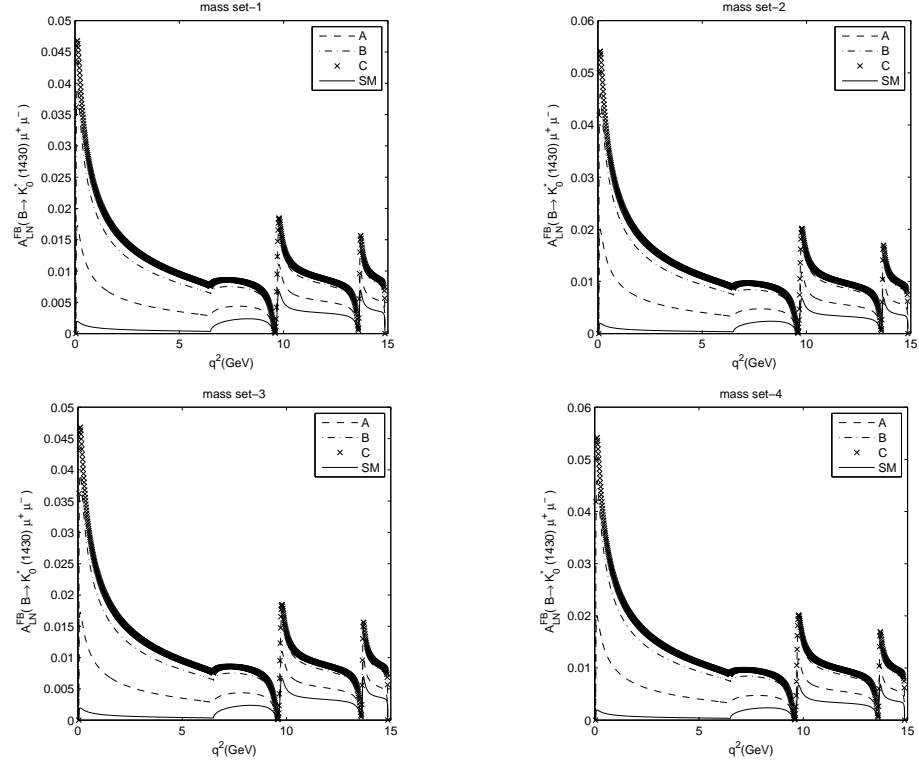


FIG. 3: The dependence of the \mathcal{A}_{FB}^{LN} polarization on q^2 and the three typical cases of 2HDM, i.e. cases A, B and C and SM for the μ channel of $\bar{B} \rightarrow \bar{K}_0^*$ transition for the mass sets 1, 2, 3 and 4.

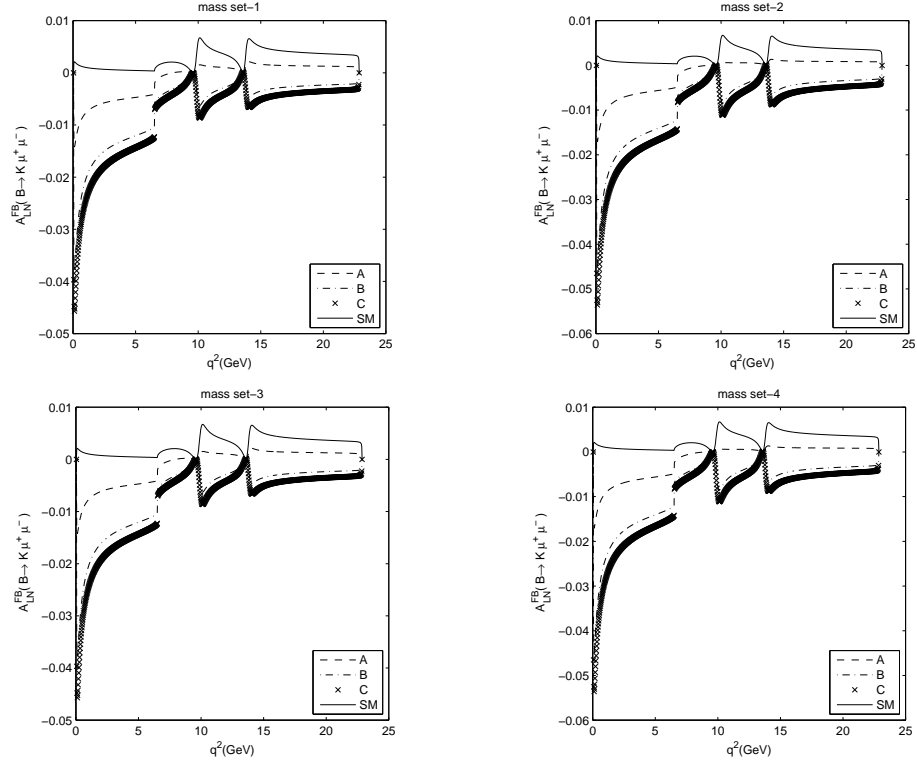


FIG. 4: The dependence of the \mathcal{A}_{FB}^{LN} polarization on q^2 and the three typical cases of 2HDM, i.e. cases A, B and C and SM for the μ channel of $\overline{B} \rightarrow \overline{K}$ transition for the mass sets 1, 2, 3 and 4.

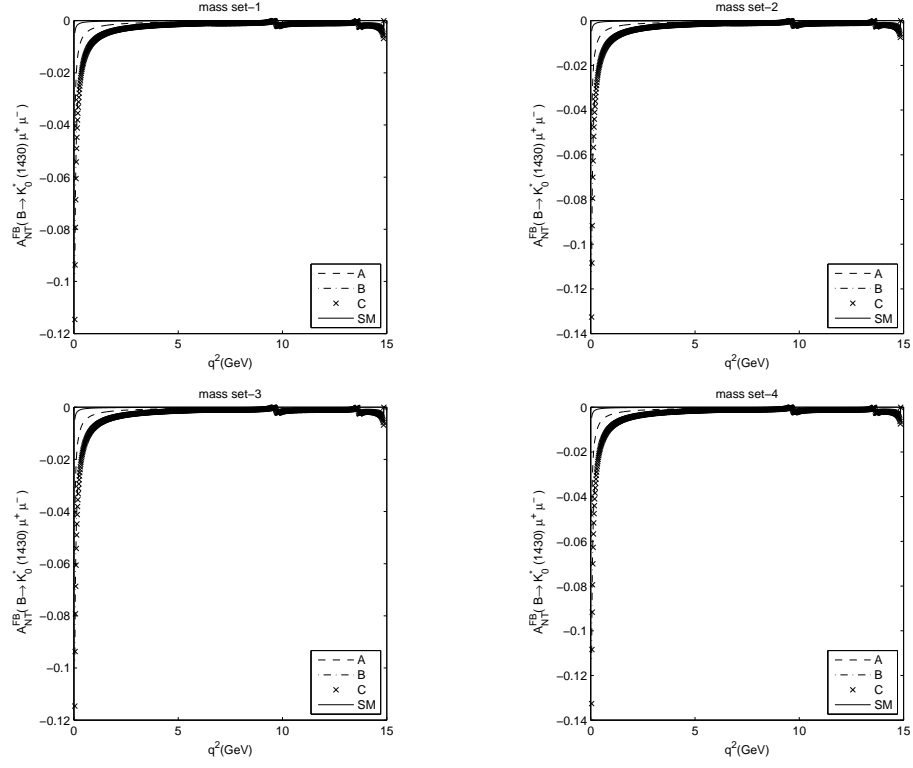


FIG. 5: The dependence of the \mathcal{A}_{FB}^{NT} polarization on q^2 and the three typical cases of 2HDM, i.e. cases A, B and C and SM for the μ channel of $\bar{B} \rightarrow \bar{K}_0^*$ transition for the mass sets 1, 2, 3 and 4.

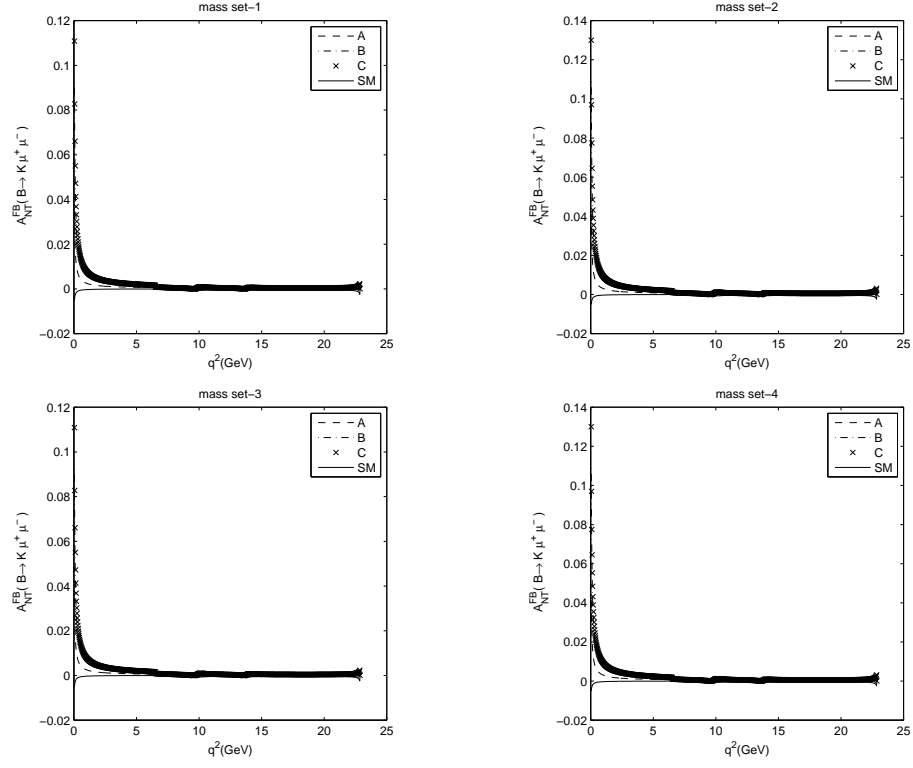


FIG. 6: The dependence of the \mathcal{A}_{FB}^{NT} polarization on q^2 and the three typical cases of 2HDM, i.e. cases A, B and C and SM for the μ channel of $\bar{B} \rightarrow \bar{K}$ transition for the mass sets 1, 2, 3 and 4.

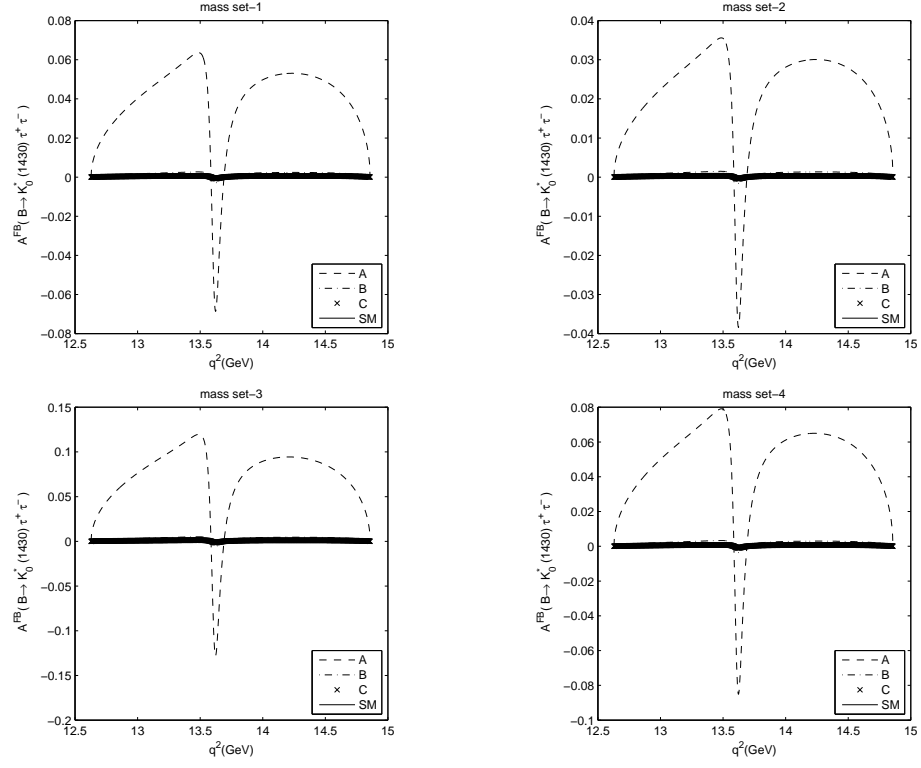


FIG. 7: The dependence of the \mathcal{A}_{FB} polarization on q^2 and the three typical cases of 2HDM, i.e. cases A, B and C and SM for the τ channel of $\bar{B} \rightarrow \bar{K}_0^*$ transition for the mass sets 1, 2, 3 and 4.

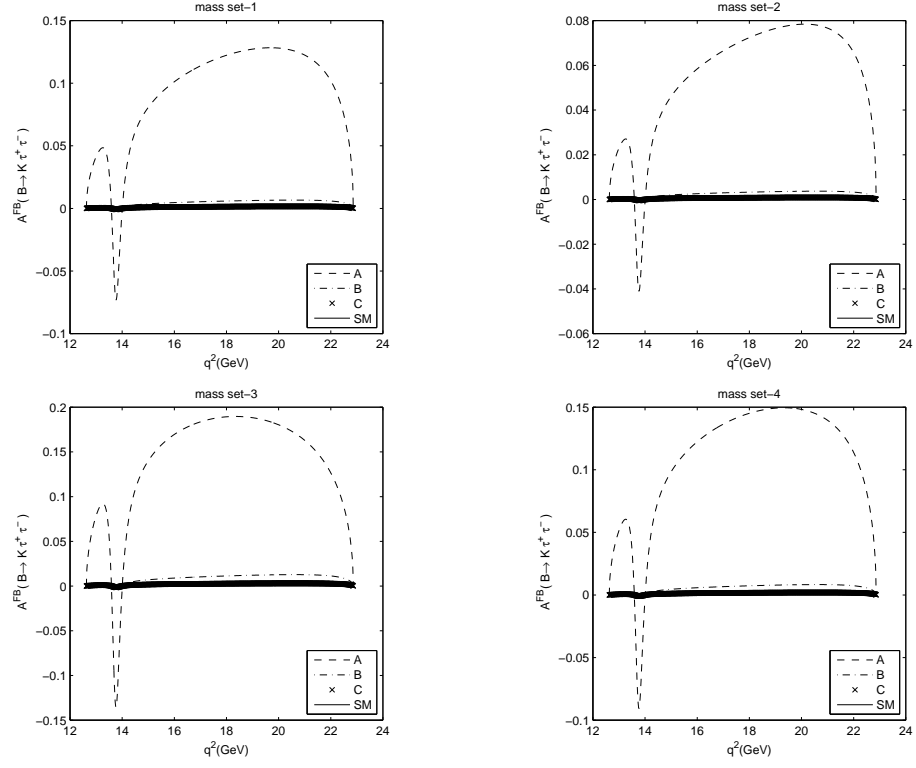


FIG. 8: The dependence of the \mathcal{A}_{FB} polarization on q^2 and the three typical cases of 2HDM, i.e. cases A, B and C and SM for the τ channel of $\bar{B} \rightarrow \bar{K}$ transition for mass sets 1, 2, 3 and 4.

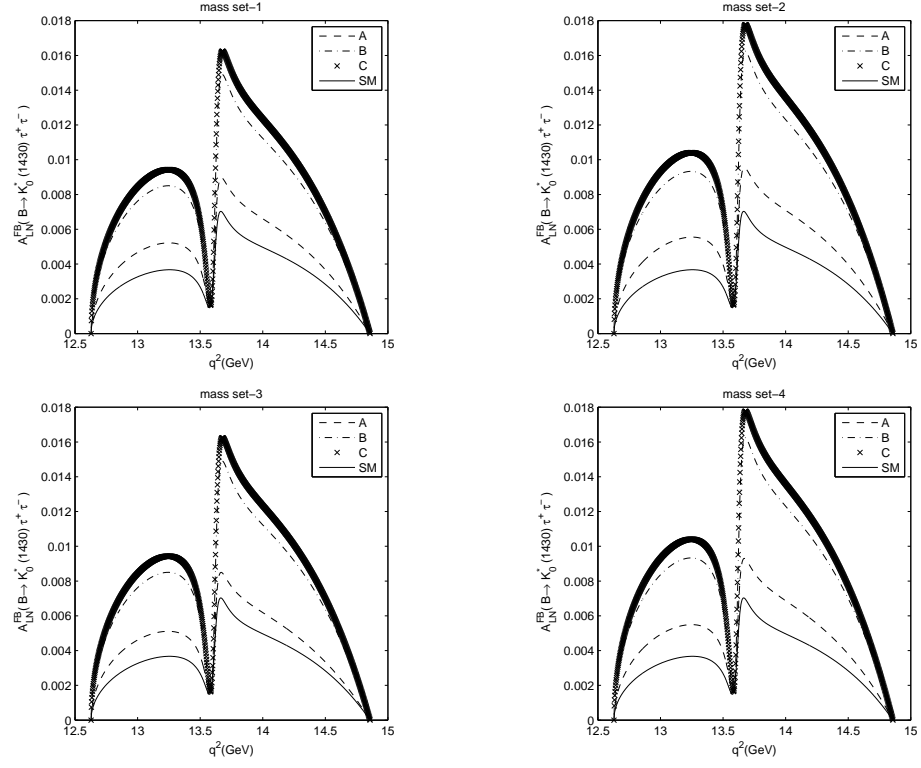


FIG. 9: The dependence of the A_{LN} polarization on q^2 and the three typical cases of 2HDM, i.e. cases A, B and C and SM for the τ channel of $\overline{B} \rightarrow \overline{K}_0^*$ transition for the mass sets 1, 2, 3 and 4.

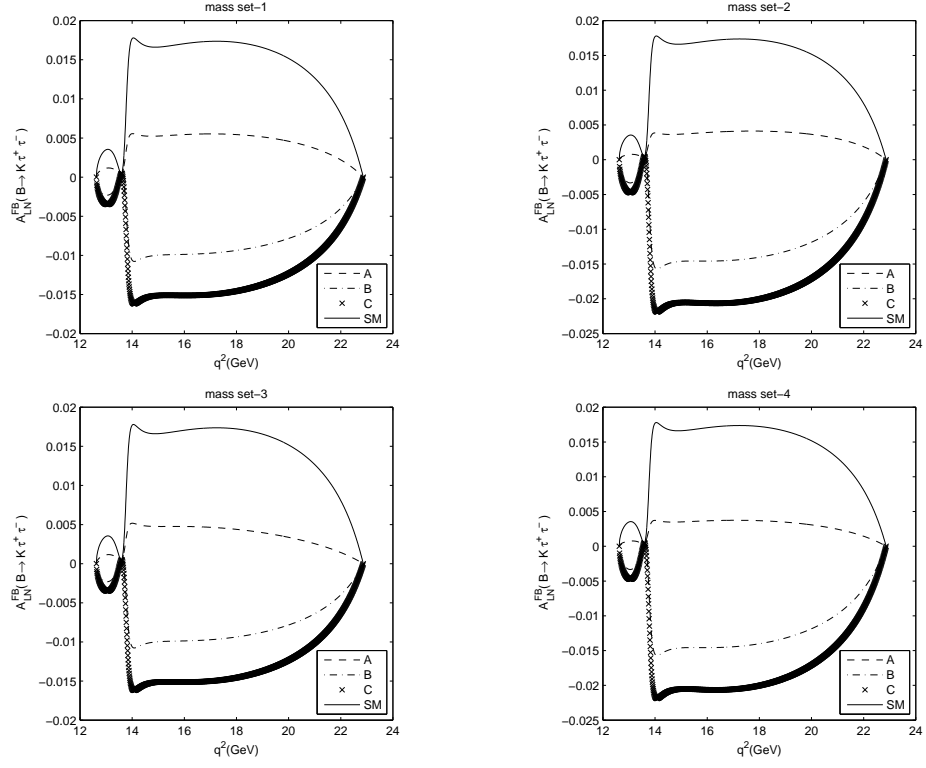


FIG. 10: The dependence of the A_{LN} polarization on q^2 and the three typical cases of 2HDM, i.e. cases A, B and C and SM for the τ channel of $\overline{B} \rightarrow \overline{K}$ transition for the mass sets 1, 2, 3 and 4.

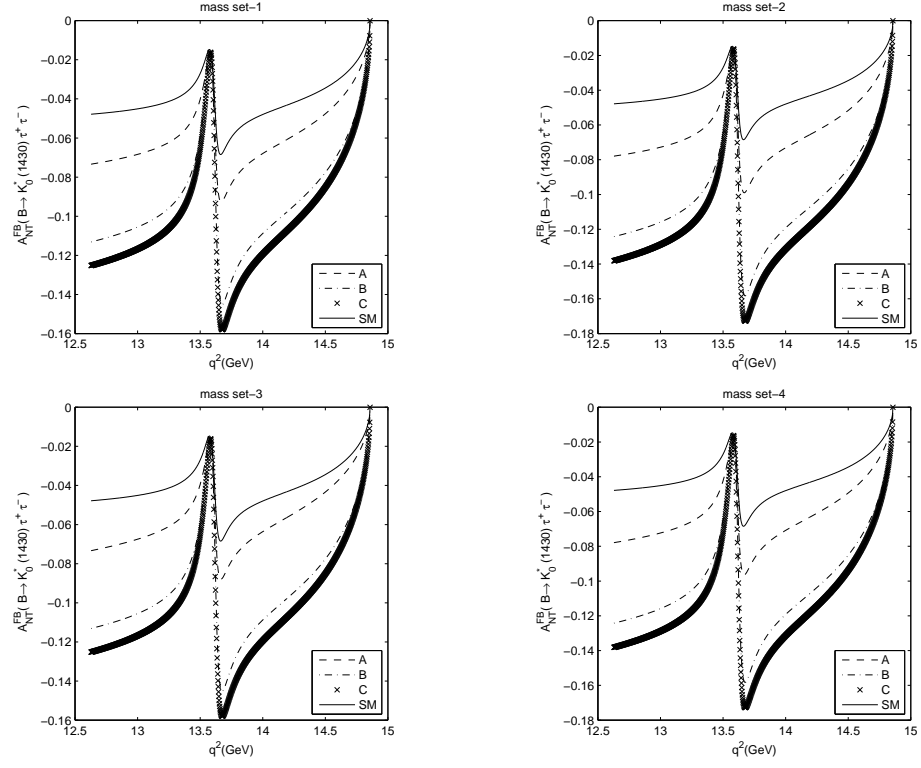


FIG. 11: The dependence of the A_{NT} polarization on q^2 and the three typical cases of 2HDM, i.e. cases A, B and C and SM for the τ channel of $\overline{B} \rightarrow \overline{K}_0^*$ transition for the mass sets 1, 2, 3 and 4.

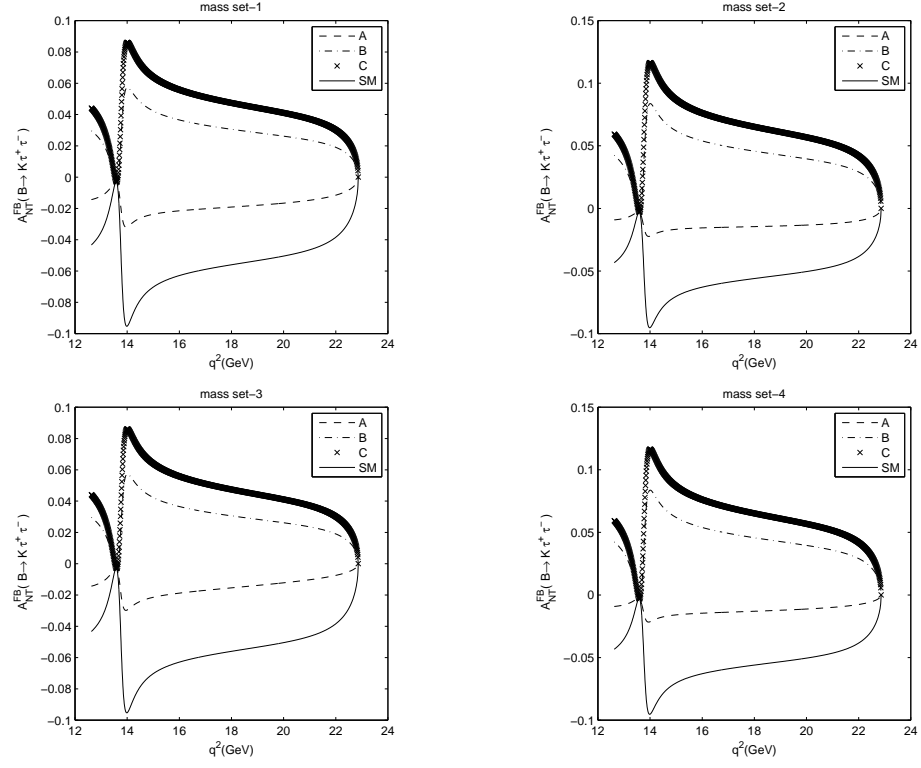


FIG. 12: The dependence of the A_{NT} polarization on q^2 and the three typical cases of 2HDM, i.e. cases A, B and C and SM for the τ channel of $\overline{B} \rightarrow \overline{K}$ transition for the mass sets 1, 2, 3 and 4.